A stoichiometric producer-grazer model incorporating the effects of excess food-nutrient content on consumer dynamics

Angela Peace [a,*], Yuqin Zhao [a], Irakli Loladze [b], James J. Elser [c], Yang Kuang [a,d]

[a] School of Mathematical and Statistical Science, Arizona State University, Tempe, AZ 85287-1804, USA
[b] 4000 S 80th St., Lincoln, NE 68506, USA
[c] School of Life Sciences, Arizona State University, Tempe, AZ 85287-4501, USA
[d] Department of Mathematics, Faculty of Science, King Abdulaziz University, Jeddah 21589, Saudi Arabia

ABSTRACT

There has been important progress in understanding ecological dynamics through the development of the theory of ecological stoichiometry. For example, modeling under this framework allows food quality to affect consumer dynamics. While the effects of nutrient deficiency on consumer growth are well understood, recent discoveries in ecological stoichiometry suggest that consumer dynamics are not only affected by insufficient food nutrient content (low phosphorus (P): carbon (C) ratio) but also by excess food nutrient content (high P:C). This phenomenon is known as the *stoichiometric knife edge*, in which animal growth is reduced not only by food with low P content but also by food with high P content, and needs to be incorporated into mathematical models. Here we present a Lotka–Volterra type model to investigate the growth response of *Daphnia* to algae of varying P:C ratios capturing the mechanism of the stoichiometric knife edge.

© 2013 Elsevier Inc. All rights reserved.

1. Introduction

Recent advances towards the understanding of ecological interactions have been made through the development of the theory of ecological stoichiometry [1]. By considering the balance of multiple chemical elements in ecological interactions, this theory provides new constraints and mechanisms that can be formulated into mathematical models. These stoichiometric models incorporate the effects of both food quantity and food quality into a single framework that produces rich dynamics [2–11]. One of these models formulated by Loladze et al. [2] describes a two-dimensional Lotka–Volterra type model of the first two trophic levels of a food chain (producer-grazer). This model, called the LKE model [12], incorporates the fact that both producer and grazer are chemically heterogeneous organisms. Specifically, it explicitly tracks the amount of two essential elements, carbon (C) and phosphorus (P), in each trophic level. It allows the phosphorus to carbon ratio (P:C) of the producer to vary above a minimum value, which effectively brings food quality into the model. The production efficiency of the consumer is reduced when this producer P:C value becomes low. The LKE model assumes the producer is optimal food for the grazer if its P:C ratio is equal to or greater than the P:C of the grazer, thus

incorporating the effects of low nutrient food content on grazer dynamics.

Thus, low nutrient food content causes a nutrient deficiency in grazers, the consequences of which are relatively well understood and modeled [2,13–15]. However, recent reported empirical data suggest that grazer dynamics are also affected by *excess* food nutrient content [16,17]. This phenomenon, called the *stoichiometric knife edge* reflects a reduction in animal growth not only by food with low P content but also by food with excessively high P content. Although the effects of excess nutrients have recently been receiving attention and there are several examples reporting the knife edge phenomenon for a variety of grazers (*Daphnia*, snails, insects, fish) [12,16–18], there is still little known about the general shape of the relationship between grazer growth rate and food P:C ratio. The shape of this curve may vary among different consumers. The recent data on this phenomenon motivate us to rethink our notion of optimal food. The "stoichiometric knife edge" implies that optimal food should no longer be considered just as that with sufficient nutrient content, which just accounts for avoiding deficiencies, but instead as a balanced nutrient content, avoiding both deficient and excess nutrient food content. While the effects of low food nutrient content have been incorporated into stoichiometric food web models, the model presented in this paper is the first to incorporate the effects of excess nutrient content. It describes an ecological system of algae (producer) and *Daphnia* (grazer), building on the structure of the

LKE model. The model was briefly introduced by Elser et al.[12]; here we give more details of the model formulation and provide analytical and numerical analysis to gain insight into the dynamics of the system and their implications.

2. Mathematical model

The model aims to capture the dynamics of the stoichiometric knife edge. One possible mechanism that may cause the observed reduction in growth is the animal's feeding behavior. Plath and Boersma [19] suggested that *Daphnia* may follow a simple feeding rule: *eat until you get enough P, then stop.* High P content of food causes the animal to strongly decrease their ingestion rate, perhaps leading to insufficient C intake and thus decreased growth rate. In other words, the satiation level of *Daphnia* is dictated by P. Here we use this hypothesis to form our model.

2.1. Model construction

We start with the stoichiometric producer-grazer LKE model [2]

$$\frac{dx}{dt} = bx\left(1 - \frac{x}{\min(K, (P - \theta y)/q)}\right) - f(x)y \tag{1a}$$

$$\frac{dy}{dt} = \hat{e}\min\left(1, \frac{Q}{\theta}\right)f(x)y - dy \tag{1b}$$

where

$$Q = \frac{P - \theta y}{x}$$

describes the variable P quota of the producer. Here $x(t)$ is the biomass of the producer, $y(t)$ is the biomass of the grazer, b is the maximum growth rate of producer, K is the producer carrying capacity, P is the total phosphorus in the system, θ is the grazer's constant P:C, q is the producer minimal P:C, $\hat{e}$ is the maximum production efficiency, and d is the grazer loss rate. The grazer's ingestion rate, $f(x)$ is taken to be a monotonic increasing and differentiable function, $f'(x) \geqslant 0$. $f(x)$ is saturating with $\lim_{x \to \infty} f(x) = \hat{f}$. The model makes the following three assumptions.

A1: The total mass of phosphorus in the entire system is fixed, i.e., the system is closed for phosphorus with a total of P (mg P/L).
A2: P:C ratio in the producer varies, but it never falls below a minimum q (mg P/mg C); the grazer maintains a constant P:C, θ (mg P/mg C).
A3: All phosphorus in the system is divided into two pools: phosphorus in the grazer and phosphorus in the producer.

In order to incorporate the dynamics of the knife edge, a fourth assumption is needed. The hypothesis claims the ingestion rate of the grazer depends on the P content of the producer.

A4: The grazer ingests P up to the rate required for its maximal growth but not more.

This assumption leads to a new expression for the grazer ingestion rate. Note that $f(x)$ is the grazer ingestion rate and Q is the P quota of the producer; thus the grazer would ingest P at rate $f(x)Q$ if its ingestion is never capped by the P content of the producer. However, the grazer's maximal possible growth rate expressed in P units is $\hat{f}\theta$. Using these two quantities, we define the grazer satiation level (GSL) as the ratio of $f(x)Q$ to $\hat{f}\theta$. If $GSL < 1$, then the grazer ingests at its usual $f(x)$ rate. But if $GSL \geqslant 1$, then the grazer ingests at the rate $\frac{\hat{f}\theta}{Q}$. This way the grazer's rate of P ingestion is capped at $(\frac{\hat{f}\theta}{Q})Q = \hat{f}\theta$.

We incorporate the assumption A4 into a new ingestion rate as follows:

$$u(x, y) = \begin{cases} f(x) & \text{for } f(x)Q < \hat{f}\theta \\ \frac{\hat{f}\theta}{Q} & \text{for } f(x)Q > \hat{f}\theta \end{cases} = \min\left\{f(x), \frac{\hat{f}\theta}{Q}\right\}$$

The grazer's production efficiency is also modified to incorporate the effect of mandatory C losses to metabolic costs, mainly to respiration, on the post-ingested food quality. Similar to the LKE, the grazer growth rate may be limited by P; however, if P is in excess, the growth rate may be limited by the amount of available C. Q is actually the P:C ratio of the producer before ingestion. A portion of this ingested C is required for metabolic costs such as respiration. $\hat{e}$ is the maximal production efficiency in terms of carbon so that $\frac{Q}{\hat{e}}$ is the P:C ratio of the post-ingested producer representing the amount of P and C available for growth (Fig. 1). When $\frac{Q}{\hat{e}} < \theta$, there is not excess P and the grazer's growth rate is determined by the P content of the producer. The grazer ingests $u(x, y)Q$ units of P, and the grazer's growth rate, $g(x, y)$, satisfies $g(x, y)\theta = u(x, y)Q$. On the other hand, when $\frac{Q}{\hat{e}} > \theta$, there is excess P. In this situation, the grazer's growth is no longer limited by P, but by the amount of available C. The grazer ingests $u(x, y)$ units of C and $u(x, y)\hat{e}$ units of C are available for growth. The growth rate then satisfies $g(x, y) = u(x, y)\hat{e}$. The grazer's biomass growth rate is defined.

$$g(x, y) = \begin{cases} \frac{Q}{\theta}u(x, y) & \text{for } \frac{Q}{\hat{e}} < \theta \\ \hat{e}u(x, y) & \text{for } \frac{Q}{\hat{e}} > \theta \end{cases}$$

$$= \min\left\{\hat{e}, \frac{Q}{\theta}\right\}u(x, y) = \min\left\{\hat{e}, \frac{Q}{\theta}\right\}\min\left\{f(x), \frac{\hat{f}\theta}{Q}\right\}.$$

Since $\hat{e}f(x) < \hat{f}$, we see that

$$g(x, y) = \min\left\{\hat{e}f(x), \frac{Q}{\theta}f(x), \hat{e}\frac{\hat{f}\theta}{Q}, \hat{f}\right\} = \min\left\{\frac{Q}{\theta}f(x), \hat{e}\frac{\hat{f}\theta}{Q}, \hat{e}f(x)\right\}.$$

Biologically, this translates into three cases in which growth is determined by energy limitation ($\hat{e}f(x)$), P limitation ($\frac{Q}{\theta}f(x)$), and P in excess ($\hat{e}\hat{f}\frac{\theta}{Q}$).

The result is the following modified version of LKE:

$$\frac{dx}{dt} = bx\left(1 - \frac{x}{\min(K, (P - \theta y)/q)}\right) - \min\left\{f(x), \frac{\hat{f}\theta}{Q}\right\}y \tag{2a}$$

$$\frac{dy}{dt} = \min\left\{\hat{e}f(x), \frac{Q}{\theta}f(x), \hat{e}\hat{f}\frac{\theta}{Q}\right\}y - dy \tag{2b}$$

Where $Q = \frac{P - \theta y}{x}$. It is worth mentioning that although the above model modifies the grazer ingestion and growth rate functions of the LKE model, no new model parameters have been introduced.
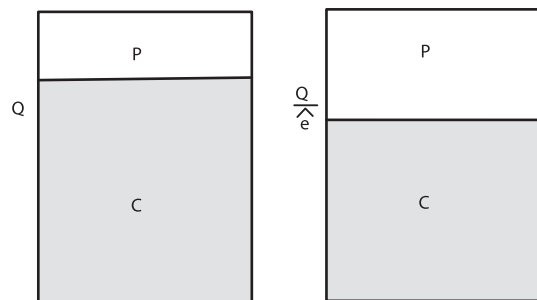

Fig. 1. This diagram depicts the carbon costs of respiration of the grazer. The left side presents the P:C of the producer prior to ingestion. Since some of the ingested C is used for respiration the P:C available for consumer growth is higher. The right figure depicts the post-ingested producer P:C, available for grazer growth.

2.2. Model analysis

Here we present a basic analysis of the model verifying the boundedness and invariance of the solution. We also develop some criteria to determine the local stability of equilibria.

Lemma 2.2.1. *The model, given in System (2) is well defined as $x \to 0$*

Proof. Since,

$$\frac{dx}{dt} = bx\left(1 - \frac{x}{\min\{K, \frac{P-\theta y}{q}\}}\right) - \min\left\{f(x), \frac{\hat{f}\theta}{Q}\right\}y$$

$$= bx\left(1 - \frac{x}{\min\{K, \frac{P-\theta y}{q}\}}\right) - \min\left\{f(x), \frac{\hat{f}\theta x}{P-\theta y}\right\}y,$$

$x'(t)$ is well defined at $x \to 0$.

$$\frac{dy}{dt} = \begin{cases} \hat{e}f(x)y - dy & \text{if } \hat{e}f(x) < \frac{Q}{\theta}f(x), \hat{e}f(x) < \hat{e}\hat{f}\frac{\theta}{Q} \\ \frac{Q}{\theta}f(x)y - dy = \frac{f(x)}{x}\frac{(P-\theta y)}{\theta}y - dy & \text{if } \frac{Q}{\theta}f(x) < \hat{e}f(x), \frac{Q}{\theta}f(x) < \hat{e}\hat{f}\frac{\theta}{Q} \\ \hat{e}\hat{f}\frac{\theta}{Q}y - dy = \hat{e}\hat{f}\frac{\theta x}{P-\theta y}y - dy & \text{if } \hat{e}\hat{f}\frac{\theta}{Q} < \hat{e}f, \hat{e}\hat{f}\frac{\theta}{Q} < \frac{Q}{\theta}f(x) \end{cases}$$

$y'(t)$ is well defined at $x \to 0$. □

Lemma 2.2.2. *Solutions with initial conditions in the open rectangle $\{(x,y) : 0 < x < k = \min\{K, \frac{P}{q}\}, 0 < y < \frac{P}{\theta}\}$ remain there for all future time.*

Proof. Assume there exists a time t_1 such that a trajectory with initial conditions in the rectangle $(0,k) \times (0, \frac{P}{\theta})$ crosses a boundary of the rectangle for the first time. The following cases prove the lemma by contradiction.

Case 1 left boundary: $x(t_1) = 0$. Let $\bar{f} = f'(0) = \lim_{x\to 0}\frac{f(x)}{x}$ and $\bar{y} = \max_{t\in[0,t_1]}y(t) < \frac{P}{\theta}$

$$x' = \left[b\left(1 - \frac{x}{\min\{K, \frac{P-\theta y}{q}\}}\right) - \min\left\{\frac{f(x)}{x}, \frac{\hat{f}\theta}{P-\theta y}\right\}y\right]x$$

$$\geq \left[b\left(1 - \frac{x}{\min\left\{K, \frac{P-\theta y}{q}\right\}}\right) - \min\left\{\bar{f}, \frac{\hat{f}\theta}{P-\theta y}\right\}y\right]x$$

$$\geq \left[b\left(1 - \frac{k}{\min\{K, \frac{P-\theta \bar{y}}{q}\}}\right) - \min\left\{\bar{f}, \frac{\hat{f}\theta}{P-\theta \bar{y}}\right\}\bar{y}\right]x = \alpha x.$$

Where α is a constant. Thus $x(t) \geq x(0)e^{\alpha t}$. This implies that $x(t_1) \geq x(0)e^{\alpha t_1} > 0$. This contradicts $x(t_1) = 0$ and proves that no such trajectory can reach this boundary.

Case 2 right boundary: $x(t_1) = k$.

$$x' = bx\left(1 - \frac{x}{\min\{K, \frac{P-\theta y}{q}\}}\right) - \min\left\{f(x), \frac{\hat{f}\theta}{Q}\right\}y$$

$$\leq bx\left(1 - \frac{x}{\min\left\{K, \frac{P-\theta y}{q}\right\}}\right) \leq bx\left(1 - \frac{x}{\min\left\{K, \frac{P}{q}\right\}}\right) = bx\left(1 - \frac{x}{k}\right)$$

Then $x(t) < k$ by the standard comparison argument, thus no trajectory can reach this boundary.

Case 3 bottom boundary: $y(t_1) = 0$.

$$y' = \min\left\{\hat{e}f(x), \frac{Q}{\theta}f(x), \hat{e}\hat{f}\frac{\theta}{Q}\right\}y - dy \geq -dy$$

This implies that $y(t_1) \geq y(0)e^{-dt_1} > 0$. This contradicts $y(t_1) = 0$ and proves that no such trajectory can reach this boundary.

Case 4 top boundary: Assume $y(t_1) = \frac{P}{\theta}$, and $0 < y(t) < \frac{P}{\theta}$ for $0 \leq t < t_1$. Then

$$y' = \min\left\{\hat{e}f(x), \frac{Q}{\theta}f(x), \hat{e}\hat{f}\frac{\theta}{Q}\right\}y - dy \leq \min\left\{\hat{e}f(x), \frac{Q}{\theta}f(x), \hat{e}\hat{f}\frac{\theta}{Q}\right\}y$$

$$\leq \frac{Q}{\theta}f(x)y = \frac{\frac{P}{\theta} - y}{x}f(x)y = \frac{f(x)}{x}\left(\frac{P}{\theta} - y\right)y \leq \bar{f}\left(\frac{P}{\theta} - y\right)y$$

$$= \bar{f}\frac{P}{\theta}y\left(1 - \frac{y}{P/\theta}\right)$$

The standard comparison argument yields a contradiction, $y(t) < \frac{P}{\theta}$ for $0 \leq t \leq t_1$. □

Lemma 2.2.3. *Solutions with initial conditions in the open trapezoid (or triangle if $K \geq \frac{P}{q}$) $\{(x,y) : 0 < x < k = \min\{K, \frac{P}{q}\}, 0 < y < \frac{P}{\theta}, qx + \theta y < P\}$ remain there for all future time.*

Proof. Based on the previous Lemma, we only have to prove $qx + \theta y < P$ for all future time. Assume that $qx(t_1) + \theta y(t_1) = P$ and $qx(t) + \theta y(t) < P$ for $0 \leq t < t_1$. Then $x(t_1) = \frac{P-\theta y(t_1)}{q}$ and $Q(t_1) = \frac{P-\theta y(t_1)}{x(t_1)} = q$. It is easy to see that $qx'(t_1) + \theta y'(t_1) \geq 0$.

$$x'(t_1) = bx(t_1)\left(1 - \frac{x(t_1)}{\min\left\{K, \frac{P-\theta y(t_1)}{q}\right\}}\right)$$

$$- \min\left\{f(x(t_1)), \frac{\hat{f}\theta x(t_1)}{P-\theta y(t_1)}\right\}y(t_1)$$

$$\leq bx(t_1)\left(1 - \frac{x(t_1)}{\frac{P-\theta y(t_1)}{q}}\right) - \min\left\{f(x(t_1)), \frac{\hat{f}\theta}{q}\frac{x(t_1)}{\frac{P-\theta y(t_1)}{q}}\right\}y(t_1)$$

$$= bx(t_1)\left(1 - \frac{x(t_1)}{x(t_1)}\right) - \min\left\{f(x(t_1)), \frac{\hat{f}\theta}{q}\frac{x(t_1)}{x(t_1)}\right\}y(t_1)$$

$$= -\min\left\{f(x(t_1)), \frac{\hat{f}\theta}{q}\right\}y(t_1)$$

$$y'(t_1) = \min\left\{\hat{e}f(x(t_1)), \frac{Q(t_1)}{\theta}f(x(t_1)), \hat{e}\hat{f}\frac{\theta}{Q(t_1)}\right\}y(t_1) - dy(t_1)$$

$$= \min\left\{\hat{e}, \frac{Q(t_1)}{\theta}\right\}\min\left\{f(x(t_1)), \frac{\hat{f}\theta}{Q(t_1)}\right\}y(t_1) - dy(t_1)$$

$$= \min\left\{\hat{e}, \frac{q}{\theta}\right\}\min\left\{f(x(t_1)), \frac{\hat{f}\theta}{q}\right\}y(t_1) - dy(t_1)$$

$$< \frac{q}{\theta}\min\left\{f(x(t_1)), \frac{\hat{f}\theta}{q}\right\}y(t_1)$$

$$qx'(t_1) + \theta y'(t_1) < -q\min\left\{f(x(t_1)), \frac{\hat{f}\theta}{q}\right\}y(t_1)$$

$$+ q\min\left\{f(x(t_1)), \frac{\hat{f}\theta}{q}\right\}y(t_1) = 0$$

This contradicts the assumption $qx'(t_1) + \theta y'(t_1) \geq 0$. □

Therefore, the solutions of system (2) are confined to a bounded region; that is, initial conditions that are outside of this boundary are biologically meaningless. To investigate the equilibria we first rewrite system (2) in the following form.

$$\frac{dx}{dt} = xF(x,y) \tag{3a}$$

$$\frac{dy}{dt} = yG(x,y) \tag{3b}$$

where

$$F(x,y) = b\left(1 - \frac{x}{\min(K,(P-\theta y)/q)}\right) - \min\left\{\frac{f(x)}{x}, \frac{\hat{f}\theta}{P-\theta y}\right\}y \quad (4a)$$

$$G(x,y) = \min\left\{\hat{e}f(x), \frac{Q}{\theta}f(x), \hat{e}\hat{f}\frac{\theta}{Q}\right\} - d \quad (4b)$$

2.3. Boundary equilibria

Consider the system,

$$x' = xF(x,y) = 0 \quad (5a)$$
$$y' = yG(x,y) = 0 \quad (5b)$$

There are two equilibria on the boundary, $E_0 = (0,0)$ and $E_1 = (k,0)$. The Jacobian of above system (5) is

$$J = \begin{vmatrix} F(x,y) + xF_x(x,y) & xF_y(x,y) \\ yG_x(x,y) & G(x,y) + yG_y(x,y) \end{vmatrix}.$$

The local stability of $E_0 = (0,0)$ is determined by the Jacobian in the following form,

$$J(E_0) = \begin{vmatrix} b & 0 \\ 0 & -d \end{vmatrix}.$$

The determinant is negative and the eigenvalues have different signs. Therefore E_0 is always an unstable saddle.

The local stability of $E_1 = (k,0)$ is determined by the Jacobian in the following form,

$$J(E_1) = \begin{vmatrix} -b & kF_y(k,0)) \\ 0 & G(k,0) \end{vmatrix}.$$

The stability of E_1 depends on the sign of $G(k,0)$. If $G(k,0)$ is positive, then E_1 is an unstable saddle. If $G(k,0)$ is negative, then E_1 is a locally asymptotically stable node.

2.4. Interior equilibria

To investigate the interior equilibria the phase plane is divided into three biologically significant regions by the two lines $\hat{e} = \frac{q}{\theta}$ and $f(x) = \frac{\hat{f}\theta}{Q}$. The following lemma shows the line $f(x) = \frac{\hat{f}\theta}{Q}$ lies beneath the line $\hat{e} = \frac{Q}{\theta}$.

Lemma 2.4.1. If $\hat{e} > \frac{Q}{\theta}$ then $f(x) < \frac{\hat{f}\theta}{Q}$.

Proof. Assume $\hat{e} > \frac{Q}{\theta}$. Since $\hat{e} < 1$ and $\hat{f} \geqslant f(x)$
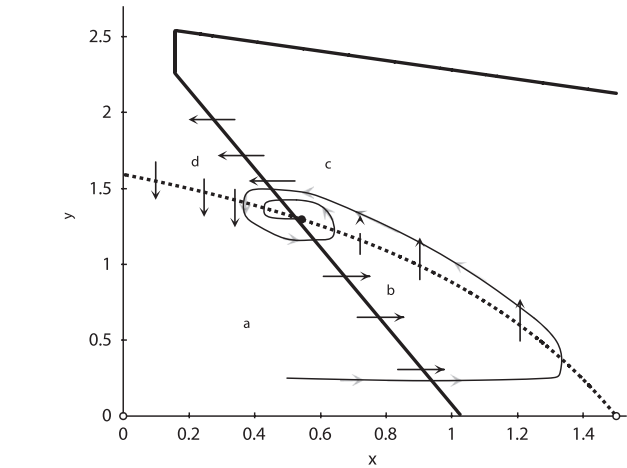
Fig. 3. This direction field analysis shows that a trajectory in region a must flow into region b, then into region c, then into region d, and finally back into region a as it approaches the locally asymptotically stable equilibrium (x^*, y^*). Therefore (x^*, y^*) is a stable spiral. The dynamics of the system experience damped oscillations as it approaches (x^*, y^*).

Table 1
Model parameters.

Parameter		Value
P	Total Phosphorus	0.03–0.2 mg P/L
$\hat{e}$	Maximal production efficiency	0.8
b	Maximal growth rate of producer	1.2 days^{-1}
d	Grazer loss rate	0.25 days^{-1}
θ	Grazer constant P:C	0.03 (mgP)/(mgC)
q	Producer minimal P:C	0.0038 (mgP)/(mgC)
c	Maximal ingestion rate of the grazer	0.81 days^{-1}
a	Half saturation of the grazer ingestion response	0.25 mg C/L
K	Producer carrying capacity	1.5 mg C/L

$$\frac{Q}{\theta} < \hat{e} < 1 \leqslant \frac{\hat{f}}{f(x)}$$

thus $f(x) < \frac{\hat{f}\theta}{Q}$ $\quad \square$

Fig. 2(c) shows the three regions. Region I is defined by $\hat{e} < \frac{Q}{\theta}$ and $f(x) < \frac{\hat{f}\theta}{Q}$. This represents the cases where P is neither limiting nor in excess. Region II is defined by $\hat{e} > \frac{Q}{\theta}$; here, growth is limited by a deficiency of P. Region III is defined by $\hat{e} < \frac{Q}{\theta}$ and $f(x) > \frac{\hat{f}\theta}{Q}$,
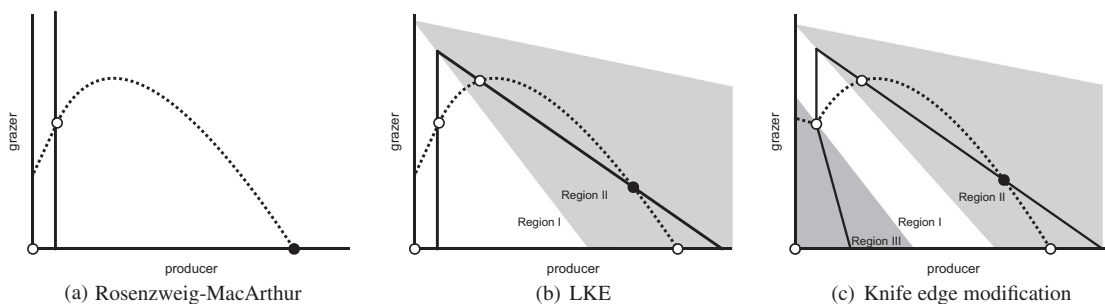
Fig. 2. Phase planes for the (a) classical Rosenzweig–MacArthur Lotka–Volterra model, (b) stoichiometric LKE model, and (c) stoichiometric LKE model modification with the knife-edge. Here we compare the grazer nullclines for these three models. The classical Lotka–Volterra grazer nullcline is a vertical line. The stoichiometric LKE model breaks the grazer nullcline into two segments. This divides the phase plane into two regions; region I, where grazer growth is determined by food quantity and region II, where grazer growth is determined by food with limiting nutrients. Finally the modified model takes into account excess food nutrient content. The grazer nullcline is divided into three segments, breaking the phase plane into three regions. This new region III is where grazer growth is limited by excess food nutrient content.

where P is in excess and reduces grazer growth. Loladze et al. [2] developed a simple graphical test that determines the local stability of the interior equilibria of the LKE system using the slopes of the nullclines determined by the sign of the partial derivatives of F and G. ($-F_x/F_y$ defines the slope of the producer nullcline and $-G_x/G_y$ defines the slope of the grazer nullcline.) We present similar results for the modified system.

The partial derivatives of F and G satisfy,

$$F_x = \frac{\partial F}{\partial x} = \begin{cases} -\frac{b}{\min\left(K, \frac{P-\theta y}{q}\right)} - \left(\frac{f(x)}{x}\right)' y & \text{if } f(x) < \frac{\hat{f}\theta}{Q} \\ -\frac{b}{\min\left(K, \frac{P-\theta y}{q}\right)} < 0 & \text{if } f(x) > \frac{\hat{f}\theta}{Q} \end{cases}$$

$$F_y = \frac{\partial F}{\partial y} = \begin{cases} -\frac{f(x)}{x} < 0 & \text{if } f(x) < \frac{\hat{f}\theta}{Q}, K < \frac{P-\theta y}{q} \\ -\frac{Ph}{(P-\theta y)^2} < 0 & \text{if } f(x) > \frac{\hat{f}\theta}{Q}, K < \frac{P-\theta y}{q} \\ -\frac{bxq\theta}{(P-\theta y)^2} - \frac{f(x)}{x} < 0 & \text{if } f(x) < \frac{\hat{f}\theta}{Q}, K > \frac{P-\theta y}{q} \\ -\frac{bxq\theta}{(P-\theta y)^2} - \frac{Ph}{(P-\theta y)^2} < 0 & \text{if } f(x) > \frac{\hat{f}\theta}{Q}, K > \frac{P-\theta y}{q} \end{cases}$$

$$G_x = \frac{\partial G}{\partial x} = \begin{cases} \hat{e}f'(x) > 0 & \text{if } \hat{e}f(x) < \frac{Q}{\theta}f(x), \hat{e}f(x) < \hat{e}\hat{f}\frac{\theta}{Q} \\ \frac{P-\theta y}{\theta}\left(\frac{f(x)}{x}\right)' < 0 & \text{if } \frac{Q}{\theta}f(x) < \hat{e}f(x), \frac{Q}{\theta}f(x) < \hat{e}\hat{f}\frac{\theta}{Q} \\ \hat{e}\hat{f}\frac{\theta}{P-\theta y} > 0 & \text{if } \hat{e}\hat{f}\frac{\theta}{Q} < \hat{e}f(x), \hat{e}\hat{f}\frac{\theta}{Q} < \frac{Q}{\theta}f(x) \end{cases}$$

$$G_y = \frac{\partial G}{\partial y} = \begin{cases} 0 & \text{if } \hat{e}f(x) < \frac{Q}{\theta}f(x), \hat{e}f(x) < \hat{e}\hat{f}\frac{\theta}{Q} \\ -\frac{f(x)}{x} < 0 & \text{if } \frac{Q}{\theta}f(x) < \hat{e}f(x), \frac{Q}{\theta}f(x) < \hat{e}\hat{f}\frac{\theta}{Q} \\ \frac{\hat{e}\hat{f}x\theta^2}{(P-\theta y)^2} > 0 & \text{if } \hat{e}\hat{f}\frac{\theta}{Q} < \hat{e}f(x), \hat{e}\hat{f}\frac{\theta}{Q} < \frac{Q}{\theta}f(x) \end{cases}$$

We denote an interior equilibrium as $E^* = (x^*, y^*)$, where $F(x^*, y^*) = 0 = G(x^*, y^*)$. The Jacobian at (x^*, y^*) is

$$J(E^*) = \begin{vmatrix} x^*F_x(x^*, y^*) & x^*F_y(x^*, y^*)) \\ y^*G_x(x^*, y^*) & y^*G_y(x^*, y^*) \end{vmatrix}.$$

The stability can be determined from the signs of the determinant, $x^*y^*(F_xG_y - F_yG_x)$ and the trace, $x^*F_x + y^*G_y$. The analysis is done for each of the regions separately.

1. Suppose (x^*, y^*) lies in region I, $\hat{e} < \frac{Q}{\theta}$ and $f(x) < \frac{\hat{f}\theta}{Q}$. Here $F_y < 0, G_x > 0$, and $G_y = 0$. The determinant is positive.

$$\text{sign}(\text{Det}(J)) = \text{sign}(-F_yG_x) > 0.$$

$$\text{sign}(\text{Tr}(J)) = \text{sign}(F_x) = \text{sign}(-F_x/F_y).$$

Since $-F_x/F_y$ is the slope of the producer nullcline, (x^*, y^*) is locally asymptotically stable if the producer nullcline is declining. If the nullcline is increasing then the equilibrium is a repeller.

2. Suppose (x^*, y^*) lies in region II, $\hat{e} > \frac{Q}{\theta}$. Here $F_y < 0, G_x < 0$, and $G_y < 0$.

$$\text{sign}(\text{Det}(J)) = \text{sign}(F_xG_y - F_yG_x) = \text{sign}\left(\frac{F_xG_y - F_yG_x}{F_yG_y}\right)$$

$$= \text{sign}\left(-\frac{G_x}{G_y} - \left(-\frac{F_x}{F_y}\right)\right)$$

If $-\frac{G_x}{G_y} < -\frac{F_x}{F_y}$, the slope of the grazer nullcline is less that the slope of the producer nullcline, then the determinant is negative and (x^*, y^*)
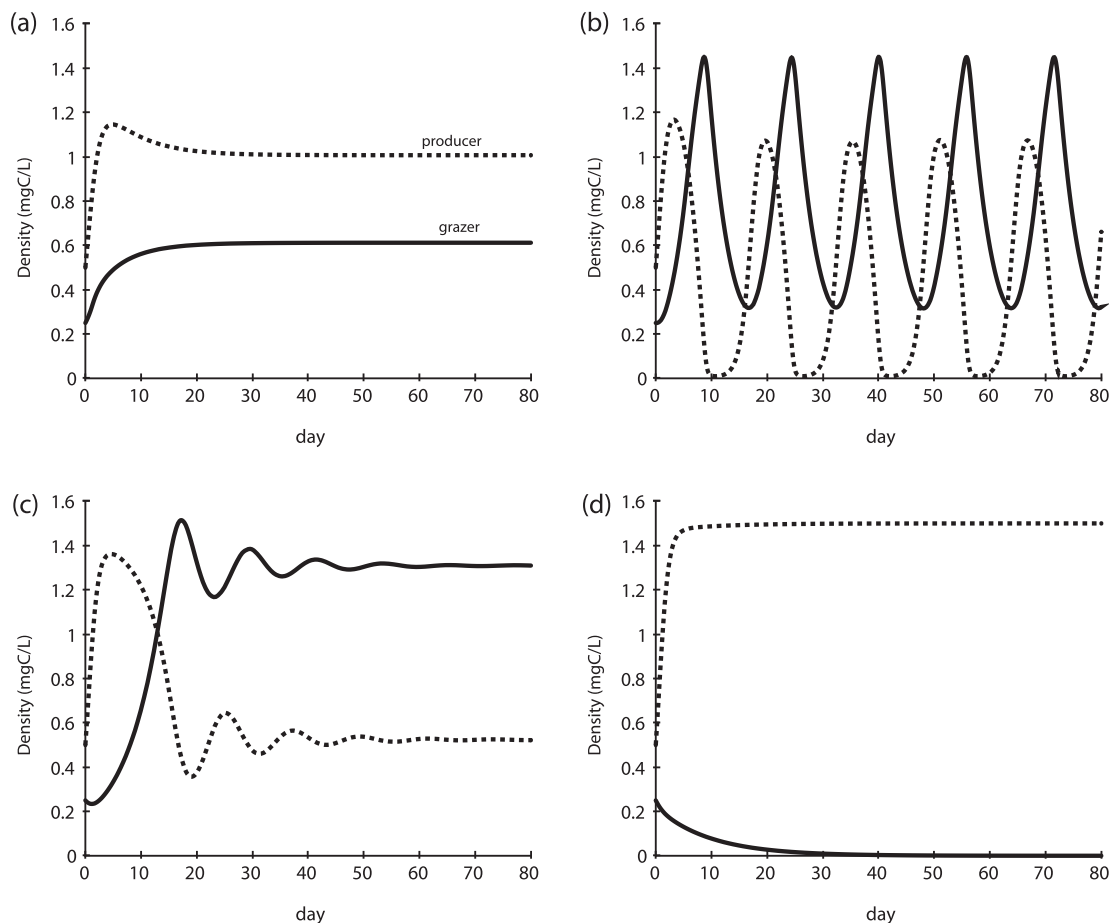

Fig. 4. Numerical simulations performed using parameters found in Table I and varying values for P, (a) low total phosphorus P = 0.03 mg P/L, (b) P = 0.05 mg P/L, (c) P = 0.08 mg P/L, (d) excess phosphorus P = 0.2 mg P/L. Panels (a) and (c) show positive stable equilibria while panel (b) captures oscillations around an unstable equilibrium. Panel (d) shows the grazer going towards extinction despite high food abundance. The extinction is caused by reduction of grazer growth due to high producer P:C.

is a saddle. If the grazer nullcline has a larger slope, then the determinant is positive.

$$F_x G_y - F_y G_x > 0 \Rightarrow F_x < \frac{F_y G_x}{G_y} < 0 \Rightarrow Tr(J) = x^* F_x + y^* G_y < 0$$

The eigenvalues for the Jacobian have negative real parts. Thus (x^*, y^*) is locally asymptotically stable.

3. Suppose (x^*, y^*) lies in region III, $\hat{e} < \frac{Q}{\theta}$ and $f(x) > \frac{\hat{f}\theta}{Q}$. Here $F_x < 0, F_y < 0, G_x > 0$, and $G_y > 0$.

$$\text{sign}(\text{Det}(J)) = \text{sign}\left(\frac{F_y G_x - F_x G_y}{F_y G_y}\right) = \text{sign}\left(-\frac{F_x}{F_y} - \left(-\frac{G_x}{G_y}\right)\right)$$

If $-\frac{F_x}{F_y} < -\frac{G_x}{G_y}$, the slope of the producer nullcline is less that the slope of the grazer nullcline, then the determinant is negative and (x^*, y^*) is a saddle. If the producer nullcline has a larger slope, then the determinant is positive. The the stability depends on the sign of trace:

$$\text{sign}(\text{Tr}(J)) = \text{sign}(x^* F_x + y^* G_y).$$

If $x^* F_x + y^* G_y > 0$, then the eigenvalues for the Jacobian have positive real parts and (x^*, y^*) is a repeller. If $x^* F_x + y^* G_y < 0$, then the eigenvalues for the Jacobian have negative real parts and (x^*, y^*) is locally asymptotically stable. Further analysis of the flow diagram shows this equilibrium is a stable spiral. The direction field on the grazer nullcline, $G(x, y) = 0$ is in the x-direction and depends on the sign of $F(x, y)$. On the grazer nullcline $x' = 0$ at (x^*, y^*), $x' > 0$ below the producer nullcline $F(x, y) = 0$, and $x' < 0$ above the producer nullcline $F(x, y) = 0$. The direction field on the producer nullcline is in the y-direction and depends on the sign of $g(x, y)$. On the producer nullcline $y' = 0$ at (x^*, y^*), $y' > 0$ to the right of the grazer nullcline $G(x, y) = 0$, and $y' < 0$ to the left of the grazer nullcline $G(x, y) = 0$. See Fig. 3 for the flow diagram.

We summarize the stability of the biologically significant equilibria in the following theorem.

Theorem 2.4.1. *There are two boundary equilibria, the origin is a saddle, the other equilibrium $E_1 = (k, 0)$ depends on the sign of $G(k, 0)$. If $G(k, 0)$ is positive this boundary equilibrium is a saddle, if $G(k, 0)$ is negative it is a locally asymptotically stable node. The stability of any interior equilibrium $E^* = (x^*, y^*)$ depends on the slopes of the producer and grazer nullclines. If $(x^*, y^*) \in$ Region I, it is locally asymptotically stable if the producer nullcline is declining and unstable if it is increasing. If $(x^*, y^*) \in$ Region II and the producer nullcline has a shallower slope than the grazer nullcline, it is locally asymptotically stable; otherwise, if the producer nullcline has a steeper slope, it is a saddle. If $(x^*, y^*) \in$ Region III and the producer nullcline has a shallower slope than the grazer nullcline, it is a saddle. If the producer nullcline has a steeper slope, the stability of (x^*, y^*) depends on the sign of $x^* F_x + y^* G_y$. If it is stable, it is a stable spiral and the system undergoes damped oscillations as it approaches (x^*, y^*).*

3. Numerical experiments

This section describes the results of numerical experiments. All simulations used the Holling type II function $f(x) = \frac{cx}{a+x}$ for the ingestion rate and the parameter values listed in Table 1. These values were also used by Loladze et al. [2] and chosen as biologically realistic values obtained from Anderson [4] and Urabe and Sterner [20].
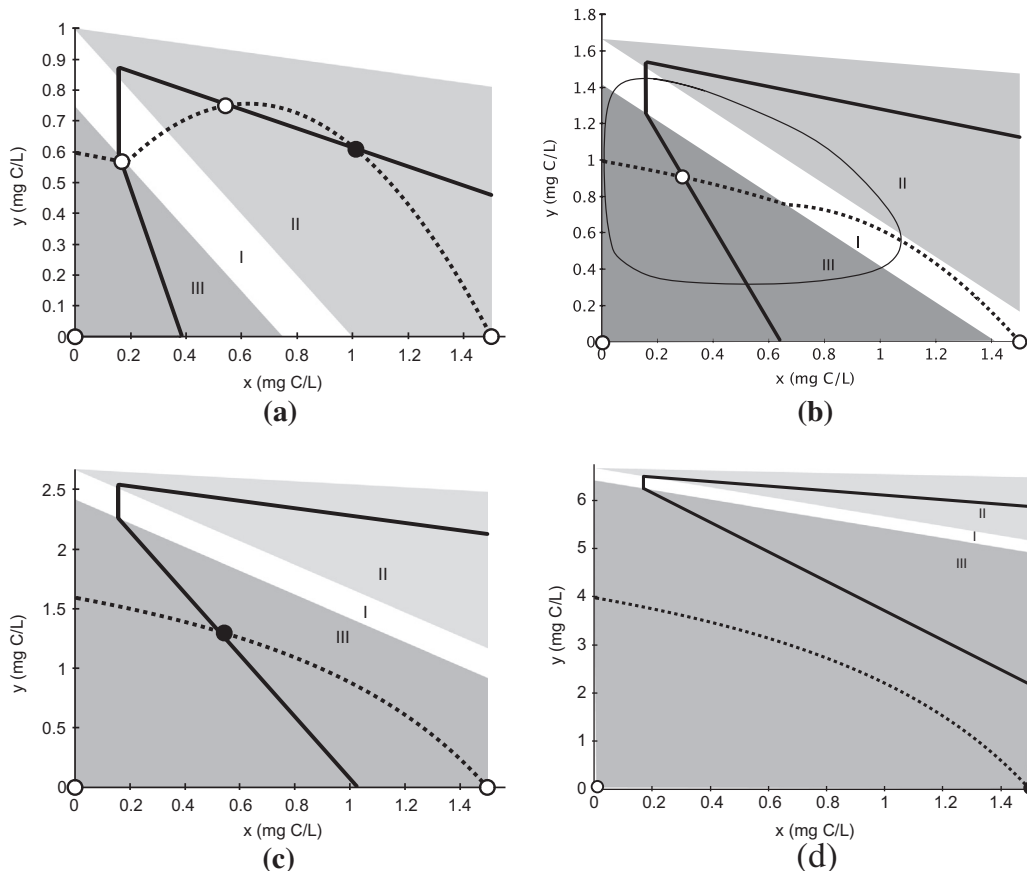

Fig. 5. Phase planes corresponding to the numerical simulations in Fig. 5, using parameters found in Table 1 and varying values for P, (a) low total phosphorus P = 0.03 mg P/L, (b) P = 0.05 mg P/L, (c) P = 0.08 mg P/L, (d) excess phosphorus P = 0.2 mg P/L. The three different regions are depicted: P is not deficient or in excess in Region I, P is limiting in Region II, and P is in excess in Region III. Open circles denote unstable equilibria and filled in circles denote stable equilibria.

The parameter P represents the total amount of phosphorus in the system. The producer takes up phosphorus; thus, the level of P affects the P:C ratio of the producer. Low values of P will result in insufficient food nutrient content for the grazer while high values of P will result in excess food nutrient content for the grazer. In our numerical experiment we increase P in an ecologically meaningful range from 0.03 to 0.2 mg P/L. When P = 0.03 mg P/L the population densities are at an equilibrium (Fig. 4(a). However, when P = 0.05 mg P/L, the population densities no longer tend to a specific value but oscillate around an unstable equilibrium (Fig. 4(b). When P = 0.08 mg P/L, the oscillations disappear and the population densities stabilize around a stable equilibrium (Fig. 4(c). Finally, for P = 0.2 mg P/L, the producer density approaches a stable positive value, but the grazer population becomes extinct (Fig. 4(d). Fig. 5 shows corresponding phase portraits for these numerical runs. The overall dynamics are similar to those of the original LKE model. However, large amounts of phosphorus in the system (P = 0.2 mg P/L) cause the grazer population to head to deterministic extinction despite the large amounts of food available. This is the result of the reduction in growth due to an excess of phosphorus in their food.

4. Model modification with bounded Quota

It is also important to note that Assumption 3 presents a problem for this model. It is assumed that all available P is in the algae; however, if the algae population is low, Q becomes unrealistically large. To improve this model more work is needed to investigate this extreme scenario of excess P with low algal density and define a maximum for the producer P quota. One possible approach to address this problem is to introduce a maximum value for Q. A modified model with a bounded quota is presented below. This modified model takes the same form as model 2 but places an

upper bound on Q. We define $\widehat{Q}$ as the maximum P:C ratio of the producer. Then Q in model 2 takes the following form.

$$Q = \min\left\{\widehat{Q}, \frac{P - \theta y}{x}\right\}$$

Assumption 2 is replaced with the following.

A2: P:C ratio in the producer varies between a minimum q (mg P/mg C) and a maximun $\widehat{Q}$ (mg P/mg C); the grazer maintains a constant P:C, θ (mg P/mg C).

Assumption 3 is no longer needed as the system allows for free P to be in the medium, outside of the grazers and producers. Simulations of the modified model are presented in Fig. 6 using parameters values in Table 1 and $\widehat{Q} = 0.07$ for varying values for P. These parameter values are the same as used in the simulations of model 2 found in Fig. 4. The dynamics are similar for these two models but there are some important differences worth noting as seen in panels (b), (c), and (d) of these Figures. In both models we see periodic oscillations around an unstable positive coexistence equilibrium for P = 0.05 mg P/L depicted in panels (b). However Fig. 6(b) shows oscillations where grazer density reaches smaller values. Fig. 4(c) shows damped oscillations towards a positive stable equilibrium whereas Fig. 6(c) shows large oscillations where the grazer density is at near zero values for a significant period of time and is very vulnerable to stochastic extinction. Fig. 4(d) shows deterministic extinction caused by reduction of grazer growth due to high producer P:C. Fig. 6(d) does not depict grazer extinction for the case of extreme excess P, but oscillations make the grazer vulnerable to stochastic extinction. This modified model, that places an upper bound on Q, appears to be more sensitive to high levels of P as the grazer density nears extinction during oscillations.
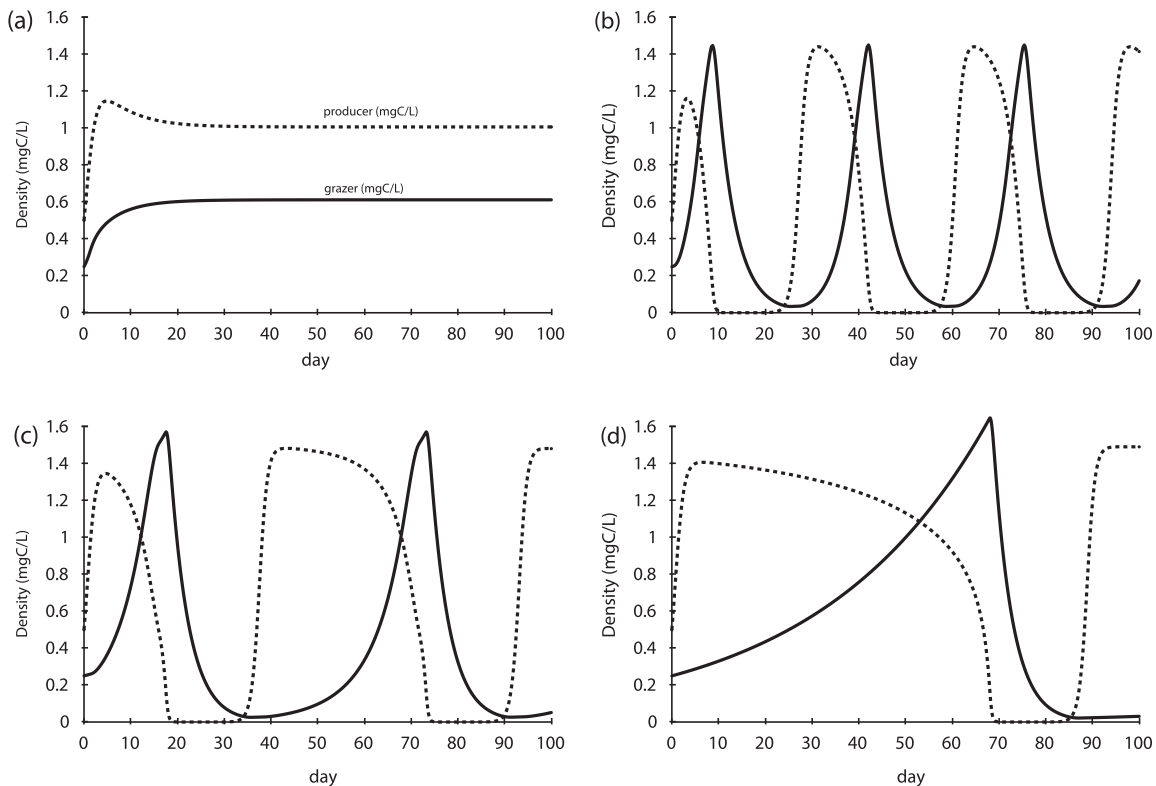

Fig. 6. Numerical simulations of the modified system performed using parameters found in Table 1 and $\widehat{Q} = 0.07$ for varying values for P, (a) low total phosphorus P = 0.03 mg P/L, (b) P = 0.05 mg P/L, (c) P = 0.08 mg P/L, (d) excess phosphorus P = 0.2 mg P/L. Grazer and producer densities (mg C/L) are given by solid and dashed lines respectively. Panel (a) shows a positive stable equilibrium while panels (b), (c), and (d) capture oscillations around unstable equilibria. As P increases, these oscillations become large in amplitude and the grazer density approaches near zero values where the grazer is very vulnerable to stochastic (but not deterministic) extinction.

5. Discussion

Ecological stoichiometry stresses the importance of incorporating the effects of food quality into food web models. While there is a clear understanding of why grazer growth is low when food nutrient content is low, there has been little insight into the consequences of reduced grazer growth when food nutrient content is high. This proposed modification of the LKE Model is the first model to incorporate the knife edge phenomenon into consumer dynamics. The dynamical consequences of the knife edge for grazers can be seen in Figs. 4(d) and 5(d). Excess P causes grazer growth to decrease and eventually leads to grazer extinction despite the high food abundance. The effects of the knife edge can also be seen in the bifurcation diagram depicted in Fig. 7. Here total phosphorus is used as a bifurcation parameter. As excess phosphorus is introduced into the system, a limit cycle emerges by Hopf bifurcation, then this limit cycle collapses by saddle-node bifurcation, grazer density begins to decrease, and eventually
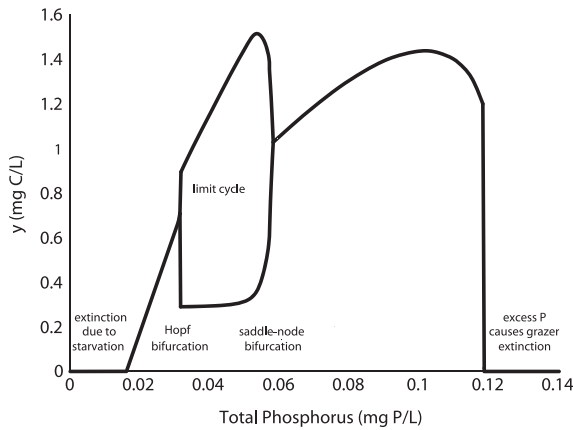

Fig. 7. A bifurcation diagram of the grazer density where total phosphorus is the bifurcation parameter. Parameter values are in Table 1 where P varies from 0 to 0.13 mg P/L and initial conditions x = 0.5 mg C/L, y = 0.25 mg C/L. For P less than 0.016 mg P/L the grazer cannot persist due to starvation. As P increases from 0.016 mg P/L to 0.031 mg P/L the grazer equilibrium increases. At P = 0.031 mg P/L this stable equilibrium loses its stability at a Hopf bifurcation. There is a limit cycle as P increases from 0.031 mg P/L to 0.058 mg P/L. When P reaches 0.058 mg P/L, the limit cycle disappears and a new stable equilibrium appears. Eventually as P increases, the grazer equilibrium begins to decreases until P = 0.118 mg P/L where the grazer can no longer persist due to excess P.

reaches deterministic extinction. To address the robustness of Fig. 7 we investigated how sensitive this bifurcation diagram is to changes in parameter values. The overall shape of the diagram is robust, however, changes in parameter values can shift the location of the Hopf and saddle-node bifurcation points along the total P axis. For example increasing b, the maximal growth rate of the producer, increases the Hopf and saddle-node bifurcation points, and shifts the diagram to the right. Increasing θ, grazer P:C, or K, producer carrying capacity, decreases the Hopf and saddle-node bifurcation points, and shifts the digram to the left.

The shape of the knife edge produced by these equations is captured in Fig. 8, where the grazer growth function, $g(x, y)$ is plotted against the P quota of the producer, Q. The left side of the curve depicts growth limitation by P and the right side shows growth decreasing due to excess P, as growth becomes limited by C because of reduced feeding rates. The shape of this curve depends on $\hat{f}\theta$, the maximum units of P ingested by each unit of grazer biomass per unit time. High values of $\hat{f}$ raise the height of the knife curve. High values of θ broaden the plateau at the peak of the grazer growth function. In reality, the value of $\hat{f}\theta$ and the shape of this curve will depend on the animal species being studied and require more detailed investigations. The theoretical knife curve (Fig. 8) as parameterized here shows that grazer growth begins to decline once the producer P:C exceeds 0.05–0.07. A relevant question is how frequently available food for zooplankton reaches levels this high. This can be assessed by considering the data compiled by Sterner et al. [21], who assembled data from published and unpublished sources consisting of 2855 observations of carbon and phosphorus ratios in suspended particulate matter from small lakes, great lakes, coastal and offshore oceans. They found that up to 10% of the data from each habitat had measurements of P:C near 0.05. Therefore, P:C values where grazer growth begins to decline due to excess P are indeed ecologically meaningful and are not infrequently observed in nature. The above model is parameterized for *Daphnia*, which have an unusually high P:C ratio ($\theta = 0.03$ [4,20]) compared to other species of zooplankton. The effects of excess P kick in when the P:C of the post ingested algae is greater than the P:C of the zooplankton ($\frac{Q}{e} > \theta$). Since other species of zooplankton have P:C ratios lower than *Daphnia* the effects of the knife edge will be seen for lower values of seston P:C; therefore such P:C values may be even more common than the 10% noted above. The issue of excess nutrients, and specifically nitrogen (N) and phosphorus excesses, becomes particularly relevant as human activities profoundly increase the inputs of these two elements into man managed and natural ecosystems. In some instances,
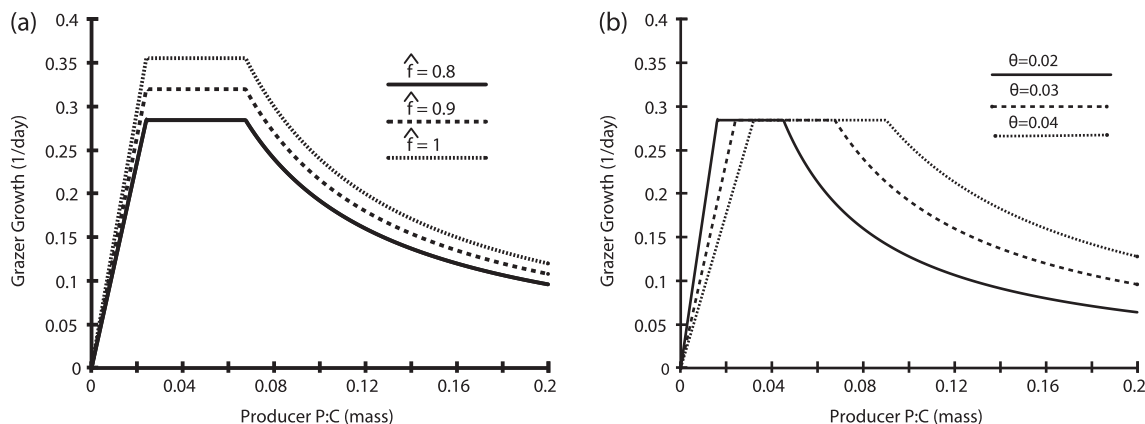

Fig. 8. Theoretical knife edge curve showing predicted dependence of grazer growth rate on producer P content for different values of $\hat{f}$ (a) and θ (b) using parameter values from Table 1. The grazer growth rate is low both when food P content is low, where growth is limited by P and when food P content is high, where P is in excess and growth is limited by C. $\hat{f}$; defined as the maximum grazer ingestion rate, controls the height of the peak of the knife curve. θ, the grazer P:C ratio controls the breadth of the plateau at the peak of the knife curve.

the human-induced N and P loads can be several magnitudes higher relative to natural levels [22,23], thus, creating ecosystem-wide states of nutrient excesses that would likely be manifested in low C:P and C:N ratios.

While our model is built on empirical work related to zooplankton dynamics and focuses on P as a key nutrient, the model likely has broader applicability. For example, this phenomenon of reduced performance on a nutrient-rich diet was also observed for locusts fed on nitrogen-fertilized plants in the study of Cease et al. [24] which provides intriguing evidence that nitrogen excess is an important nutritional factor regulating plant-insect interactions. Morehouse et al. [28] showed that high dietary P:C ratios reduce the growth rate of zebra mussels. This study shows that understanding this knife-edge phenomenon may be critical for developing sustainable land management practices.

It is important to note that the model presented here is a first attempt to capture the knife-edge in an analytically tractable form and to examine its underlying dynamical structure and implications. That is, it is an effort to examine the dynamical consequences of the knife edge for grazers. The mechanisms behind the *stoichiometric knife edge* are likely to be more complicated than a simple reduction in ingestion rate, the hypothesis we incorporated into Assumption 4. A second hypothesis is that the feeding behavior does not change but excess P may cause the animal to decrease its C absorption rate. That is, once inside the animals, C and P might compete for absorption sites and excess P may hinder C absorption. A third hypothesis is that excess P may increase metabolic costs. Respiration rate may increase due to the costs of egesting, metabolizing, and/or excreting extra P. Ultimately, the mechanisms behind the stoichiometric knife edge may reflect any combination of these different responses [12]. More experiments on respiration and feeding rates are needed to evaluate the mechanisms underlying this observed reduction in growth rate. Once we have a clearer understanding of the biology behind this phenomenon, we can modify the model to include the specific mechanisms that create it.

Another possible modification of the model is to include stage-structure. Food nutrient content potentially has a different effect on grazer growth during different stages of development. Early stages characterized by high growth rates may be especially affected by nutrient limitation [7] due to low food P content. Stoichiometric constraints indeed affect grazer growth and ontogeny [14,25]. Reproductive tissues have high contents of N and P; thus, low food nutrient content may have strong effects on reproductive output [26]. It is not clear how excess food nutrient content might affect growth rates at the various stages of the developmental cycle. Such stage-specific effects will affect population dynamics, suggesting a stage-structured model will be more appropriate. We also note the opportunity to extend this knife edge model to include more than one consumer species and to examine subsequent impacts of coexistence and exclusion, as in the analysis of Loladze et al. [10].

The analysis in this paper mainly focused on the limit sets of the model as well as the system equilibria and their stability and limit cycles, and did not address transient dynamics. Flexible algal C:P stoichiometry is likely to affect the transient behavior of producer-grazer systems [27]. Further analysis of the transient dynamics will lead to better insight and understanding of this model and yield insight into relevant ecological situations such as the initiation of spring algal blooms and subsequent grazer response and regulation.

References

[1] R. Sterner, J. Elser, Ecological Stoichiometry: The Biology of Elements from Molecules to the Biosphere, Princeton University Press, NJ, 2002.
[2] I. Loladze, Y. Kuang, J. Elser, Stoichiometry in producer-grazer systems: linking energy flow with element cycling, Bull. Math. Bio. 62L (2000) 1137.
[3] S. Diehl, S. Berger, R. Wohrl, Flexible nutrient stoichiometry mediates environmental influences on phytoplankton and its resources, Ecology 86 (11) (2005) 2931.
[4] T. Andersen, Pelagic Nutrient Cycles; Herbivores as Sources and Sinks, Springer, Berlin, 1997.
[5] D. Hessen, B. Bjerkeng, A model approach to planktonic stoichiometry and consumer-resource stability, Freshwater Biol. 38 (1997) 447.
[6] E. Muller, S. Kooijman, J. Elser, E. McCauley, Stoichiometic food quality and herbivore dynamics, Ecol. Lett. 4 (2001) 519.
[7] T. Andersen, J. Elser, D. Hessen, Stoichiometry and population dynamics, Ecol. Lett. 7 (2004) 884.
[8] J. Grover, Predation, competition, and nutrient recycling: a stoichiometric approach with multiple nutrients, J. Theor. Biol. 229 (2004) 31.
[9] S. Hall, Stoichiometrically explicit competition between grazers: species replacement, coexistence, and priority effects along resource supply gradients, Am. Nat. 164 (2004) 157.
[10] I. Loladze, Y. Kuang, J. Elser, W. Fagan, Competition and stoichiometry: coexistence of two predators on one prey, Theor. Popul. Biol. 64 (2004) 1.
[11] M. Fan, I. Loladze, Y. Kuang, J. Elser, Dynamics of a stoichiometric discrete producer-grazer model, J. Differ. Equ. Appl. 11 (2005) 347.
[12] J. Elser, I. Loladze, A. Peace, Y. Kuang, Lotka re-loaded: modeling trophic interactions under stoichiometric constraints, Ecol. Modell. 245 (2012) 3.
[13] J. Elser, K. Hayakawa, J. Urabe, Nutrient limitation reduces food quality for zooplankton: Daphnia response to seston phosphorus enrichment, Ecology 82 (2001) 898.
[14] W. Demott, R. Gulati, K. Siewertsen, Effects of phosphorus-deficient diets on the carbon and phosphorus balancance of Daphnia magna, Limnol. Oceanogr. 43 (1998) 1147.
[15] P. Frost, J. Benstead, W. Cross, H. Hillebrand, J. Larson, M. Xenopoulos, T. Yoshida, Threshold elemental ratios of carbon and phosphorus in aquatic consumers, Ecol. Lett. 9 (2006) 774.
[16] M. Boersma, J. Elser, Too much of a good thing: on stoichiometrically balanced diets and maximal growth, Ecology 87 (2006) 1325.
[17] J. Elser, J. Watts, J. Schampell, J. Farmer, Early Cambrian food webs on a trophic knife-edge? a hypothesis and preliminary data from a modern stromatolite-based ecosystem, Ecol. Lett. 9 (2006) 295.
[18] J. Elser, J. Schampel, M. Kyle, J. Watts, E. Carson, T. Dowling, C. Tang, P. Roopnarine, Reponse of grazing snails to phosphorus enrichment of modern stromatolitic microbial communities, Freshwater Biol. 50 (2005) 1826.
[19] K. Plath, M. Boersma, Mineral limitation of zooplankton: stoichiometric constraints and optimal foraging, Ecology 82 (2001) 1260.
[20] J. Urabe, R. Sterner, Regulation of herbivore growth by the balance of light and nutrients, Proc. Nat. Acad. Sci. USA 93 (1996) 8465–8469.
[21] R. Sterner, T. Andersen, J. Elser, D. Hessen, J. Hood, E. McCauley, J. Urabe, Scale-dependent carbon: nitrogen: phosphorus seston stoichiometry in marine and freshwaters, Limnol. Oceanogr. 53 (2008).
[22] J. Elser, E. Bennett, Phosphorus cycle: a broken biogeochemical cycle, Nature 478 (2011) 29.
[23] V. Smith, D. Schindler, Eutrophication science: where do we go from here?, Trends Ecol Evol. 24 (2009) 201.
[24] A. Cease, J. Elser, C. Ford, S. Hao, L. Kang, J.F. Harrison, Heavy livestock grazing promotes locust outbreaks by lowering plant nitrogen content, Science 335 (2012) 467–469.
[25] M. Villar-Argaiz, R. Sterner, Life history bottlenecks in Diaptomus clavipes induced by phosphorus-limited algae, Limnol. Oceanogr. 47 (2002) 1229.
[26] P. Frvig, D. Hessen, Allocation strategies in crustacean stoichiometry: the potential roleof phosphorus in the limitation of reproduction, Freshwater Biol. 48 (2003) 1782.
[27] C. Jager, S. Diehl, C. Matauschek, C. Klausmeier, H. Stibor, Transient dynamics of pelagic producer-grazer systems in a gradient of nutrient and mixing depths, Ecology 89 (5) (2008) 1272.
[28] R. Morehouse, A. Dzialowski, P. Jeyasingh, Impacts of excess dietary phosphorus on zebra mussels, Hydrobiologia 707 (2013) 73.